Electrospinning · Nanofiber · poly(styrene-*co*-acrylonitrile) · Hansen solubility parameter · Teas graph

Non-woven nanostructured webs of poly(styrene-*co*-acrylonitrile) (SAN) were produced by electrospinning, which are promising in advanced filtration. A range of solvents was chosen for electrospinning of SAN on the basis of Hansen's solubility parameter approach. The consequences of variation of the governing parameters on average fiber diameter and morphology of the electrospun SAN fibers were experimentally studied. Solution viscosity has the most substantial role in controlling the diameters of electrospun SAN fibers obtained using various solvents. The range of solution viscosity that can fabricate defect-free fibers is also dependent on the solvent/polymer system used.

Effekt von Lösungsmitteln auf die Elektrospinning-Lösung von Poly(styrol-*co*-acrylonitril)

Elektrospinning · Nanofaser · Poly(styrol-*co*-acrylonitril) · Hansen Löslichkeitsparameter · Teas graph

Nicht verwebte nanostrukturierte Gewebe von Poly(styrol-*co*-acrylnitril (SAN) wurden durch Elektrospinning hergestellt, welche Vorteile bei der Filtration versprechen. Eine Gruppe von Lösungsmitteln sind auf Basis des Hansen-Löslichkeitsparameteransatzes für das Elektrospinning von SAN ausgewählt worden. Die Auswirkungen einer Variation von gegebenen Parametern auf den mittleren Faserdurchmesser und auf die Morphologie der elektrogesponnenen SAN-Fasern sind experimentell untersucht worden. Die Lösungsviskosität spielt die maßgebliche Rolle zur Kontrolle der Durchmesser der elektrogesponnenen SAN-Fasern, welche mit den verschiedenen Lösungsmitteln erzielt wurden.
Die Bereich der Lösungsviskositäten, welche für die Herstellung von defektfreien Fasern einsetzbar sind, ist auch abhängig von dem eingesetzten Lösungsmittel/Polymer –System.

Figures and Tables:
By a kind approval of the authors.

Effect of Solvents on the Solution Electrospinning of Poly(styrene-*co*-acrylonitrile)

1. Introduction

During the past decades, substantial development has happened in the fabrication of functional nanofibers, which can find diverse applications in protective clothing, tissue engineering, filtration, electronics, sensors, catalysis and bioanalysis owing to their high porosity combined with significant specific dimensions and greater surface area-to-volume ratio [1-7]. Among the various fiber fabrication techniques, electrospinning seems to be the most prominent multi-disciplinary method for producing non-woven nanofibrous mats with unique structure [8]. In electrospinning, a high electrostatic force is applied across a polymer melt or solution and a collector surface, which induces the polymer solution to spray or eject in the form of charged fluid jet from the tip of a spinneret and ultrafine polymeric nanofibers deposit on the surface of the collector as a non-woven membrane [9]. Electrospun fiber morphology, texture and diameter depend on many parameters that are generally divided into three categories, such as solution parameters (solution viscosity, electrical conductivity, concentration, surface tension, and charge carried by the spinning jet), process parameters (applied voltage, solution flow rate, needle tip-to-collector distance (TCD), and diameter of the needle), and ambient parameters (relative humidity, temperature, local atmosphere flow, velocity of air, and atmosphere pressure) [10, 11]. On the other hand, the abovementioned electrospinning parameters are neither basic control factors nor are they independent of each other.

In a typical electrospinning process, solvent is an important contributor to obtain uniform, ultrafine, defect-free fibers. Some earlier works have indicated the significance and influence of the properties of solvents in polymer solution electrospinning [12-16]. In general, the properties of any solvent-polymer system can be predicted by the effectiveness of the solvent for the successful conformations of the polymer chains in the solvent. In a good solvent, the polymer chain configurations are ideal and the intermolecular interactions are favorable for the complete expansion of the polymer chains, which ultimately lead to completely random chain conformations. Therefore, the selection of solvents based on the several properties of the solvents that determine the intermolecular interactions between solvent molecules and monomer units is crucial for the optimization of electrospinning of a particular polymer.

In electrospinning process, the selection of the best solvent is advantageous in three major ways: first is to lower the concentration of the polymer in the solution since the ideal conformation of the polymer chains allows the ubiquitous chain entanglements in the solution that favor the stability of the solution droplet at the needle tip even at the low polymer concentration. When a polymer is dissolved in a good solvent, the polymer chains will be randomly oriented within the polymer solution in such a way that the chains occupy the maximum possible

Authors

T. Senthil, S. Anandhan, Mangaluru, India

Corresponding authors:
S. Anandhan
Department of Metallurgical and Materials Engineering,
National Institute of Technology Karnataka,
Surathkal, Srinivas Nagar (P.O),
Mangaluru-575025, India.
Ph: +91-824-2473762
Fax: +91-824-2474059
E-Mail: anandtmg@gmail.com, anandhan@nitk.ac.in

KGK RUBBERPOINT

Discover more interesting articles and news on the subject!

www.kgk-rubberpoint.de

Entdecken Sie weitere interessante Artikel und News zum Thema!

space, especially at a low concentration. As the solution concentration is increased further, the polymer chains repel themselves to reduce the overall energy associated with the orientation of the chains in the solution. As a result, the chains will reorient themselves and spread uniformly in the solution. If the concentration reaches a certain critical level (critical chain overlap concentration, *C**), the chains will not be able to move freely in the solution, and the motion is affected by the neighboring chains. In other words, for polymer concentrations above *C**, the chains will be entangled. *C** determines the transition of dilute to semi-dilute regimes of the polymer solution. At solution concentration above the critical entanglement concentration (C_e), the number of polymer chain entanglements significantly increases, which assists the polymer jet withstand the electric field to form bead-free fibers [17], as shown in Fig. 1. Second, the obtention of bead/defect free high aspect ratio fibers and finally, fibers with low diameters. In other words, for a good solvent, the critical concentration for the transition from electrospraying to fiber spinning will be lower than that of the solvents with moderate/poor chain conformations/entanglements. In this regard, by changing the solvent system for a polymer, different fiber morphology can be produced, such as dimpled, cup, half hollow sphere, spherical, spindle-like bead structures and continuous long fibers with smooth and porous surfaces.
The selection of the best solvents for a polymer can be carried out empirically using theoretical predictions with a considerable level of accuracy. Hansen solubility parameters can estimate a solvent's ability to interact with the polymer chains in the solvents and *vice versa*, based on the dielectric strength, the presence of polar groups, molecular weight etc [18]. In this method: initially, one has to locate the components: dispersion forces component (δ_d), the hydrogen bonding component (δ_h) and the polar force component (δ_p) of Hansen's solubility parameters of the list of solvents and the respective polymers in a Teas plot. The positions of solvent on the Teas graph are stationary and the solvents falling within the solubility region of the respective polymer, which is specified as the interaction radius, can be considered for the electrospinning. These selected polymers can be ranked again by the interaction distance, which is a measure of distance between the points representing the polymer and the solvents and the polymer [19].

Poly(styrene-*co*-acrylonitrile) (SAN) was chosen for the present study to extend the applicability of Hansen solubility parameters for the optimal selection of solvents for electrospinning; at the same time, to correlate the solvent properties with the morphology and yield of electrospun SAN fibrous/nanosized structures. SAN is a random copolymer of styrene and acrylonitrile, which exhibits exceptional properties, such as oil and chemical resistance, transparency, heat resistance, toughness and rigidity and its fibrous form is appropriate for many applications, such as catalyst immobilization, ultrafiltration of corrosive chemicals, food packaging, medical masks and air filters, etc [20]. The current focus on SAN is a step towards the electrospinning of copolymers, which has not been addressed in depth in literature [21-23].
In this study, we extensively investigated the effects of fabrication parameters in electrospinning of SAN from its eight solutions (i.e. in chloroform, tetrahydrofuran, *N,N*-dimethyl formamide, toluene, 1,2-dichloroethane, n-butanone or methyl ethyl ketone, ethylacetate, and dimethyl sulfoxide). Hansen's philosophy of solubility approach was employed to select the suitable solvents for electrospinning of SAN. Moreover, a ternary solubility diagram, namely Teas graph, was also utilized to aid the search for appropriate solvents for preparing SAN solutions. Using this Teas graph and Hansen graph, eight solvents were chosen for the electrospinning of SAN to examine the influence of variations in the concentration of solution and applied voltage on spinnability and electrospun fiber morphologies.

2. Experimental details

2.1 Materials

SAN [viscosity average molecular weight ($\bar{M}_v$): 2.46 × 10^6 (Oswald viscometry)], with an acrylonitrile content of 30 %, was obtained from Bhansali Engineering Polymers, Sirohi, Rajasthan, India. The eight solvents used in this study were chloroform (CF) (>99 %, NICE chemicals Pvt. Ltd., Kochi, India), tetrahydrofuran (THF) (>99 %, CDH Pvt. Ltd., New Delhi, India), N,N-dimethyl formamide (DMF) (>99 %, SRL Pvt. Ltd., Mumbai, India), toluene (>99 %, NICE chemicals Pvt. Ltd., Kochi, India), 1,2-dichloroethane (DCE) (>99 %, CDH Pvt. Ltd., New Delhi, India), n-butanone or methyl ethyl ketone (MEK) (>99 %, SRL Pvt. Ltd., Mumbai, India), ethylacetate (EA) (>99 %, Spectrochem Pvt. Ltd., Mumbai, India), dimethyl sulfoxide (DMSO) (>99 %, HPLC Pvt. Ltd., Mumbai, India). All these solvents were used without further purification as they were of the analytical grade. $\bar{M}_v$ of SAN was calculated using Oswald viscometry using the Mark-Kuhn-Houwink (MKH) **equation (1)**:

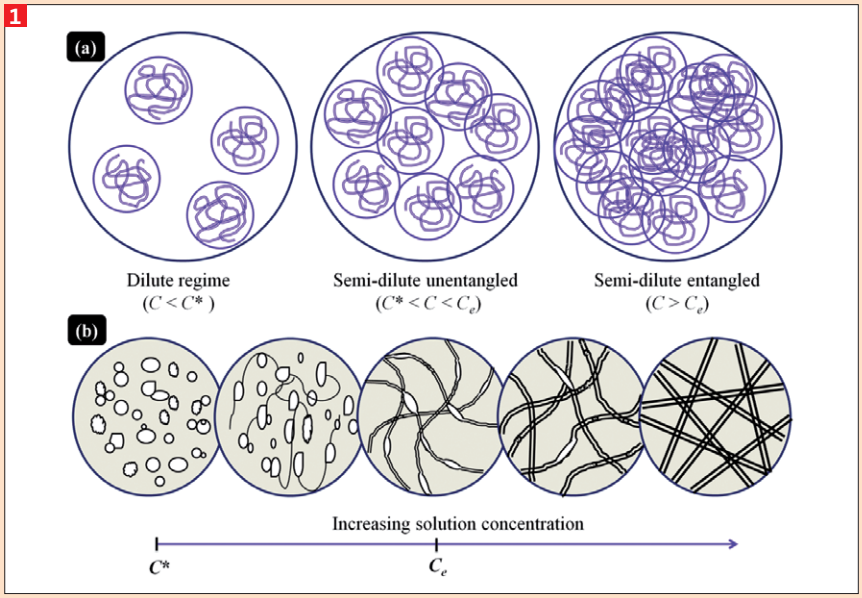

Fig. 1: (a) Physical illustration of the three solution regimes, (b) Typical change in morphology from droplets/beads through beaded fibers into ultrafine fibers occurring with increasing solution concentration.

$$([\eta] = K\,\overline{M}_v{}^{a}) \quad (1)$$

where, a = 0.62 for n-butanone as the solvent and $K = 3.6 \times 10^{-4}$ [24].

2.2 Electrospinning of SAN nanofibers

A vertical electrospinning unit was used for the electrospinning process is shown in Fig. 2. The polymer solutions of various concentrations (8, 10, 12, 15 and 20 (w/v%)) were prepared by dissolving appropriate quantities of SAN in 100 mL of CF, THF, DMF, toluene, DCE, MEK, DMSO, and EA in closed beakers at 30±3 °C using a magnetic stirrer at a mixing speed of 2000 rpm for 6h. The SAN solutions were placed into medical plastic syringes (5 mL) and then they were electrospun under a varied high DC voltages (10, 15 and 20 kV), onto aluminum foil-wrapped grounded conductive static collector (Fig. 2). The spinning solutions were delivered at a controlled flow rate of 300 µL.h^{-1} through a metallic needle; spinneret tip-to-collector distance (TCD) was 23 cm. The electrospinning equipment (ESPIN-NANO) was supplied by Physics Equipments Co., (Chennai, Tamil Nadu, India).

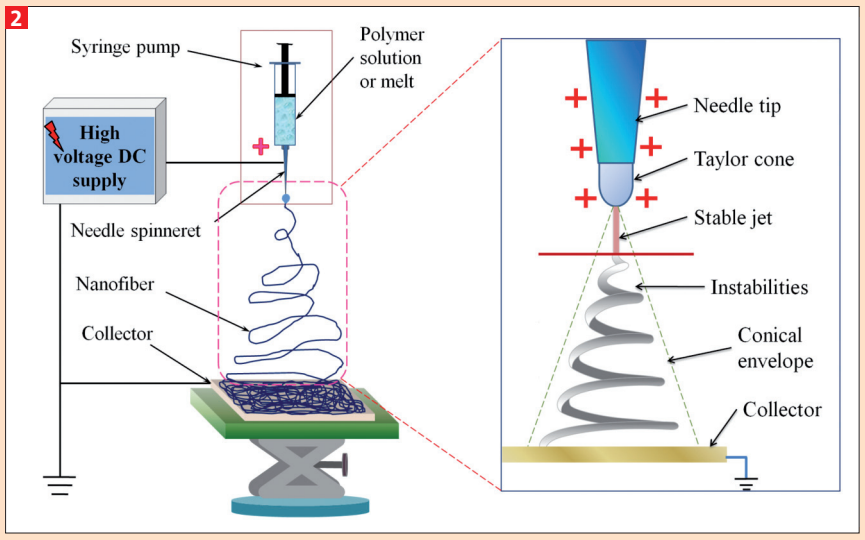

Fig. 2: Schematic of the electrospinning set-up.

2.3 Characterization

Electrical conductivities, surface tension and coefficient of viscosities of the SAN solutions were measured at 30±3 °C using a conductivity meter (EQ 667, Equip-Tronics, Mumbai, Maharashtra, India), tensiometer (SEO-DST 30M, Germany) and Brookfield digital viscometer (Model DV II, Middleboro, Massachusetts, USA), respectively. The gold sputtered electrospun SAN fibers' (sputtered by a JFC 1600 auto fine coater, JEOL, Tokyo, Japan) diameters and morphology were determined using a scanning electron microscope (JEOL-JSM-6380 LA, Japan) at an accelerating voltage of 20 kV, using secondary electrons for imaging. Moreover, the as-spun fiber images and an individual fiber diameter (i.e. an average of 6 measurements taken along the fiber axis) were analyzed and measured using Smile Shot™ software (JEOL, Tokyo, Japan). To measure the average fiber diameter ($D_{avg.}$) of the SAN fibers attained under a specific spinning

1 Physical properties of solvents used in this work

Solvents[a]	Molecular weight[b] (g/mol)	Boiling point[b] (°C)	Density[b] (g/cm^3)	Dipole moment[b] (Debye)	Dielectric constant[b]	Solubility parameter[c] (MPa)^{½}
Chloroform	119.4	61.5	1.480	1.01	4.8	18.95
Tetrahydrofuran	72.11	66.0	0.888	1.63	7.5	19.46
N,N-dimethyl formamide	73.10	154.0	0.949	3.82	37.3	24.86
Toluene	92.11	112.0	0.864	0.36	2.4	18.16
1,2-dichloroethane	98.96	84.0	1.254	2.94	10.2	20.80
n-butanone	72.11	81.0	0.805	2.76	18.5	19.05
Ethylacetate	88.10	77.1	0.901	1.78	6.0	18.15
Dimethyl sulfoxide	78.13	192.0	1.101	3.96	46.7	26.68

[a]Source: Brandrup, J., Immergut, E.H., 1989 [24] [b]Source: Smallwood, I.M., 2002 [25] [c]Source: Hansen, C.M., 2007 [18]

2 Solubility parameters of various solvents and SAN

Solvents[a]	Solubility Parameter[b] (MPa$^{1/2}$)				d*[a]	SAN solubility	Electrospinnability
	δ	δ_d	δ_p	δ_h			
Chloroform	18.95	17.8	3.1	5.7	2.56614	High	Transition
Tetrahydrofuran	19.46	16.8	5.7	8	0.66116	High	Spin (beaded fibers)
N,N-dimethyl formamide	24.86	17.4	13.7	11.3	–0.80892	High	Spin
Toluene	18.16	18	1.4	2	5.67664	High	Spin
1,2-dichloroethane	20.80	19	7.4	4.1	–1.60703	High	Transition
n-butanone	19.05	16	9	5.1	–1.11383	High	Spin
Ethylacetate	18.15	15.8	5.3	7.2	0.00729	High	Transition
Dimethyl sulfoxide	26.68	18.4	16.4	10.2	–3.15487	High	Spin
SAN (Polymer)	20.7	16.60	9.80	7.60	(4.80)	-----	-----

[a]Source: Brandrup, J., Immergut, E.H., 1989 [24] [b]Source: Hansen, C.M., 2007 [18]

condition, diameters of at least 50 fibers were measured and their average values along with standard deviations have been computed.

3. Results and Discussion

SAN solutions in eight solvents were prepared with a range of concentrations from 8 to 20 w/v% to study the effect of solvent system on the morphological characteristics of the electrospun fibers. To identify the best electrospinning solvent, at first, the common solvents for polystyrene (PS) and polyacrylonitrile (PAN) were chosen from the literature to dissolve SAN [24 & 25]. Also, the solvents were chosen based on their physical properties, to reveal the effects of solvents on the spinnability of SAN. Some important physical constants of these solvents are summarized in Table 1. The values given in Table 1 were taken from the literature [18 & 19]. The physical properties of the solvents were correlated to the spinnability of SAN in them. Dipole moment plays a prime role in determining the cohesive energy between the polymer chains and the solvents, which ultimately determines whether the solvent is good or bad for a polymer for the complete entanglement of the chains. Dielectric constant measures the net charge accumulated on the spherical droplet at the needle tip, which is a measure of the ease of fiber formation [26]. Therefore, a high dielectric constant and dipole-moment are preferred during the selection of solvents.

Solubility parameters, δ, are used to help the hunt for desirable solvents and solvent systems for a particular polymers used in solution electrospinning. Appropriate solvents were chosen, which have solubility parameters either close to or away from that of SAN (Table 2). Hansen's solubility theory [18] was used for evaluation of the solubility behaviors of these solvents. δ is of numerical significance that shows the relative solvency behavior of a particular solvent, was determined by equation (2):

$$\delta = \sqrt{E_d} = \left(\frac{\Delta H - RT}{V_m}\right)^{1/2} \qquad (2)$$

where, E_d indicates the cohesive energy density, R is the universal gas constant, V_m specifies the molar volume, T is the temperature and ΔH is the heat of vaporization [15], and the solubility parameter SI unit is $MPa^{1/2}$.

In the Hansen solubility sphere, three-dimensional (3-D) coordinate system of

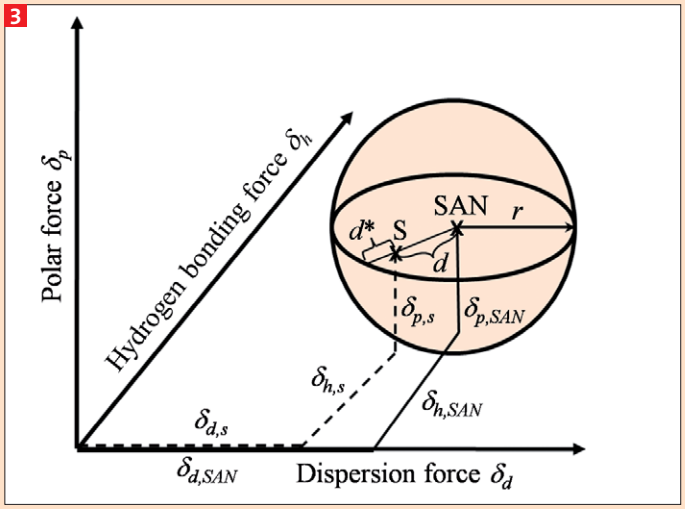

Fig. 3: Scheme of a Hansen solubility graph: *d-calculation for a single solvent.**

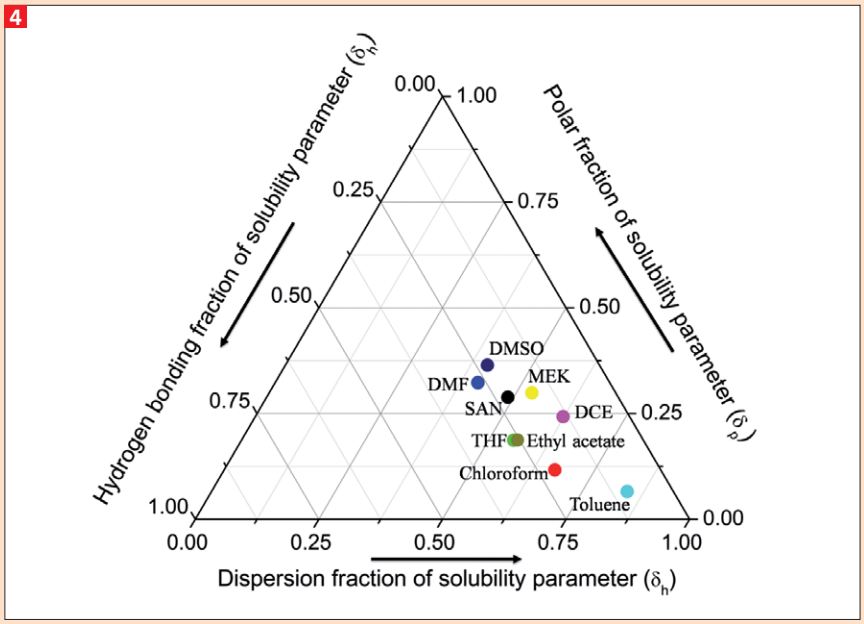

Fig. 4: Teas plot of Hansen solubility parameters for SAN solvent classes.

δ_p, δ_d, and δ_h is used to represent the spherical region surrounding the polymer where the three dimensional coordinated of the best solvent for the polymer falls. Any solvents (*S*) for which these coordinates located within the Hansen sphere can dissolve polymer (SAN) instantaneously. The interaction radius '*r*' of the SAN sphere is 4.80 $MPa^{1/2}$ [18].

$$r = \left[4\left(\delta_d - \delta_{d,SAN}\right)^2 + \left(\delta_p - \delta_{p,SAN}\right)^2 + \left(\delta_h - \delta_{h,SAN}\right)^2\right]^{1/2} \qquad (3)$$

where, $\delta_{d,SAN}$, $\delta_{p,SAN}$, $\delta_{h,SAN}$ signify the coordinates of the centre of the Hansen sphere and known by the Hansen solubility parameters of the polymer (Fig. 3), in this case SAN. The least distance between the polymer and solvent coordinates, can be calculated as,

$$d^* = r - d = r - \left[4\left(\delta_{d,s} - \delta_{d,SAN}\right)^2 + \left(\delta_{p,s} - \delta_{p,SAN}\right)^2 + \left(\delta_{h,s} - \delta_{h,SAN}\right)^2\right]^{1/2} \qquad (4)$$

where, d^* signifying the distance between the surface of the Hansen sphere and the solvent coordinates and d is the distance between the polymer and the solvent coordinates. A minimum distance between the polymer and the solvent coordinates, i.e. $d^*<0$, is expected for the best suited solvent for defect free electrospinning and high-yield of nanofibers, as shown in Table 2.

A ternary solubility diagram based on the Hansen solubility parameters, also

5

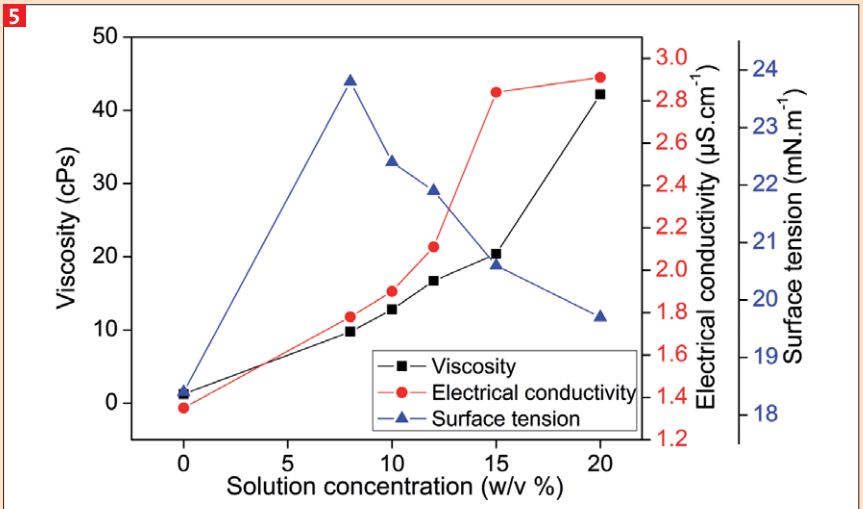

Fig. 5: Variation of coefficient of viscosity, electrical conductivity and surface tension as a function of solution concentration on SAN/CF solutions.

6

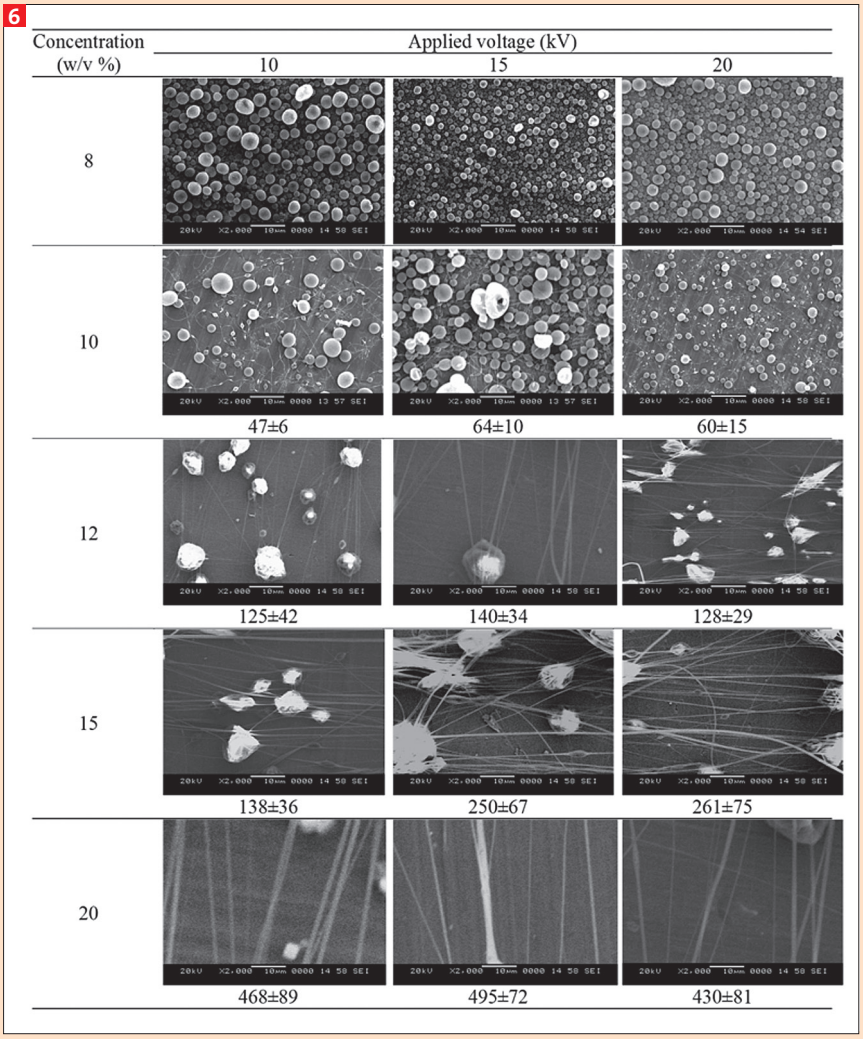

Fig. 6: Representative SEM images (magnification 2000× and scale bar = 10 µm) of SAN fibers spun from CF solutions of different concentrations (w/v %) under varying applied voltage (for a fixed flow rate of 300 µL h^{-1} and TCD of 23 cm) (The values below the SEM images show the $D_{avg.}$ and the standard deviation of fiber diameter).

known as the Teas graph, is considered to be the best and well-designed among the large diversity of solubility scales in the literature for the preparation of polymer solution, and one can make use of this for reducing the tediousness of selecting the solvent for electrospinning [27]. The axes of Teas plots δ_p, δ_d and δ_h, which are fractional coordinates, derived from the polar component δ_p, the dispersion component δ_d and the hydrogen bonding component δ_h of the solubility parameter, respectively. Any solvent can be represented by a point on Teas plot, provided that one has to know the three corresponding fractional parameters on the solvent, and also in the case of polymers.

In Teas triangle, the fractional coordinate axes have been reduced to a scale of 0-1.00. Therefore, Teas plots can be used as an easy way of spatial representation of polymers and solvents which are under consideration and the points representing the solvent in the locality of that of the polymer can be considered for electrospinning process. In this study, the criteria for the selection of the most suited solvent for electrospinning was the position of the solvent on the Teas graph, which lies in proximity to the position of a good solvent for electrospinning for SAN. Teas graph was developed for SAN based on the solubility parameter (Fig. 4) and the suitability of the SAN solutions were thoroughly examined for electrospinning. Based on the solubility principles a set of solvents were also chosen for the detailed study. The dissolution of SAN was tried in chosen solvents and electrospun to obtain nanofibers at different electrospinning conditions. The morphology of the thus obtained fibers was studied.

3.1 Electrospinning of SAN from chloroform

SAN dissolves in chloroform to produce a spinnable solution and nanofibers with different morphology can be attained by changing the electrospinning parameters. In case of SAN dissolved in chloroform, the tip of the spinneret often got clogged by the dried polymer due to the low boiling point (61.5 °C) of the solvent, as shown in Table 1. The variation of surface tension, electrical conductivity and coefficient of viscosity as a function of the SAN solutions in chloroform are shown in Fig. 5. It can be seen that both the viscosity and electrical conductivity of solution increase with increasing solu-

tion concentration. Also, the surface tension of the SAN solutions marginally decreases as their concentrations increase, which denotes that surface tension has a very slight impact on the fiber formation. In general, the relation between solution viscosity and surface tension is linear, as reported earlier for pure and mixed solution [28], the relationship is;

$$\ln\gamma = \ln A + \frac{B}{\eta} \qquad (5)$$

where, γ is the surface tension, η is the solution viscosity, A and B are the constant which depends on the nature of the polymer used.

SEM micrographs of electrospun SAN fibers are illustrated in Fig. 6. At lower concentration (8 %), mostly droplets and some short fibers with beads were observed. At the solution concentrations of 10 and 12 %, the fibers were found to have a fewer beads with a lower average fiber diameter. These droplets and beads significantly disappeared by increasing the solution concentration from 12 to 20 %. This underscores the importance of a critical solution concentration at which entanglements form to an optimum extent, which eliminates the possibility of bead formation. Relatively large diameter fibers were noticed in fibers spun at a higher concentration of 20 %. Uniformity of the electrospun SAN fibers increased with increasing applied voltage significantly (10 to 20 kV). The electrospun nanofibers produced at 20 kV have an even diameter distribution with few beaded morphology.

3.2 Electrospinning of SAN from tetrahydrofuran

Tetrahydrofuran was able to dissolve SAN to develop a spinnable solution and resulted in the formation of few incipient fibers with predominantly beads. The changes in surface tension, electrical conductivity and coefficient of viscosity as a function of the SAN solutions in THF are shown in Fig. 7. It reveals that the viscosities of the SAN solutions increase substantially with increasing polymer concentration. Besides, the surface tension gradually decreases with increasing concentration of the polymer solution. As expected, the solution often got clogged because of the low boiling point of THF (66.0 °C; Table 1). This clogging is similar to that observed for the solution of SAN in chloroform.

Figure 8 shows the SEM micrographs of the electospun SAN nanofibers attained

7

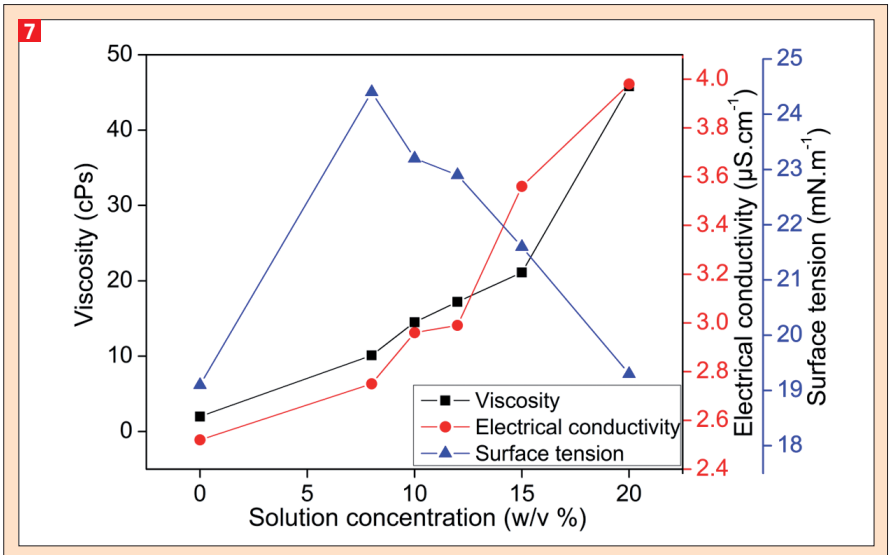

Fig. 7: Variation of coefficient of viscosity, electrical conductivity and surface tension as a function of solution concentration on SAN/THF solutions.

8

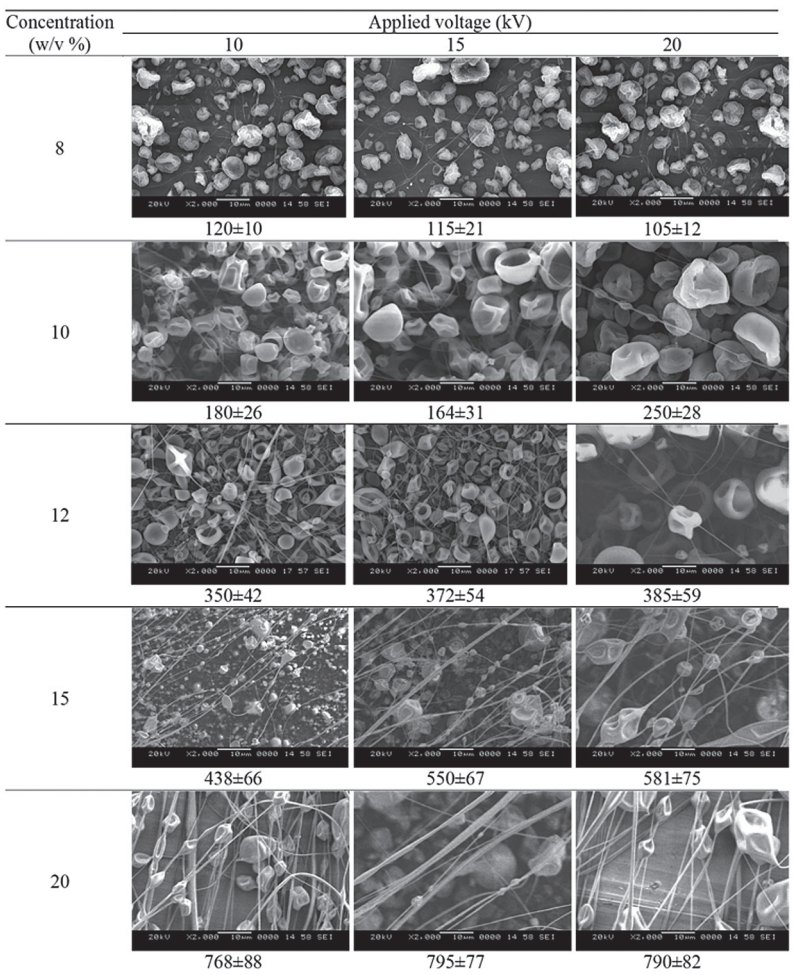

Fig. 8: Representative SEM images (magnification 2000× and scale bar = 10 µm) of SAN fibers spun from THF solutions of different concentrations (w/v %) under varying applied voltage (for a fixed flow rate of 300 µL h^{-1} and TCD of 23 cm). (The values below the SEM images show the $D_{avg.}$ and the standard deviation of fiber diameter).

9

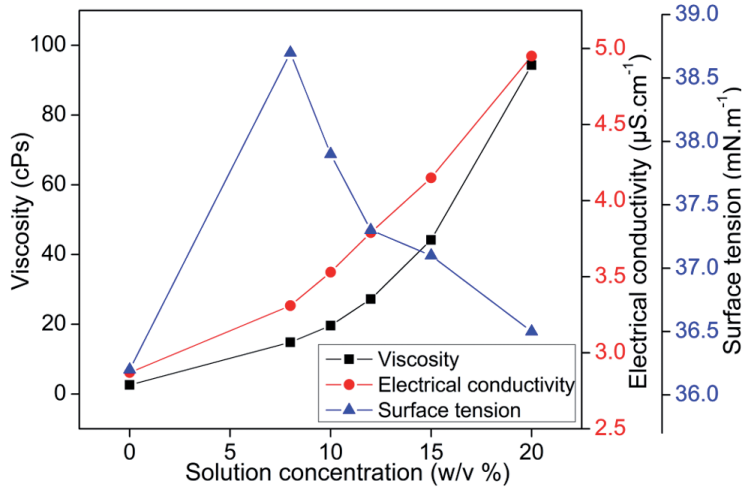

Fig. 9: Variation of coefficient of viscosity, electrical conductivity and surface tension as a function of solution concentration on SAN/DMF solutions.

10

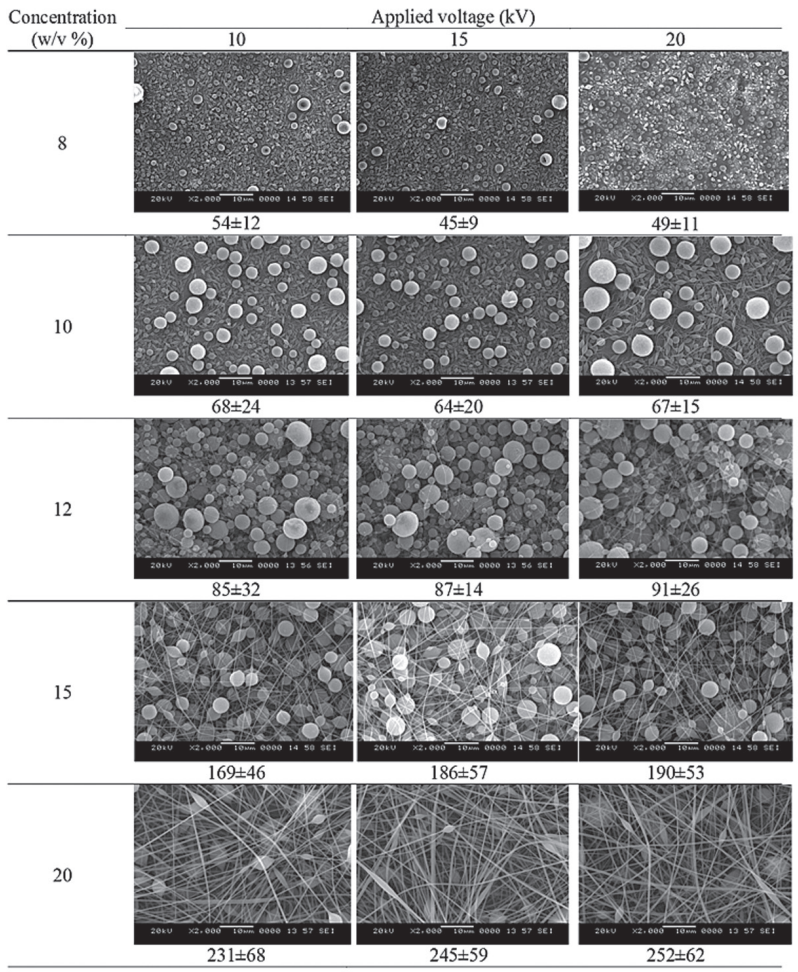

Fig. 10: Representative SEM images (magnification 2000× and scale bar = 10 μm) of SAN fibers spun from DMF solutions of different concentrations (w/v %) under varying applied voltage (for a fixed flow rate of 300 μL h^{-1} and TCD of 23 cm). (The values below the SEM images show the $D_{avg.}$ and the standard deviation of fiber diameter).

from solutions of different concentrations (ranging between 8 and 20 w/v%) under varying electrostatic field strength. It was noticed that, depending on the concentration of polymer solution, the electrospun fiber morphology reveals different trends with varied applied voltage. There was a slight change in fiber morphology with increasing applied voltage. A large number of dimple-like beads were observed at a lower concentration for both 8 and 10 % SAN solutions; however, a slight change was observed at the solution concentration of 12 %. This indicates that solution concentrations well above C_e are required to stabilize the electrospinning jet. At 15 %, the morphology changes from beads to beads on strings. When the solution concentration increases to 20 %, mixture of smooth and fewer beaded fibers were observed, which indicates that still a high enough polymer chain entanglements are needed to completely prevent the charged jet from breaking up.

3.3 Electrospinning of SAN from N,N-dimethyl formamide

N,N-dimethyl formamide was able to dissolve SAN to form a spinnable solution to produce SAN fibers. Interestingly, increasing the solution concentration also resulted in ultrafine bead-free fibers with reasonable diameters. The variations of surface tension, electrical conductivity and coefficient of viscosity as a function of the SAN solutions in DMF are shown in Fig. 9. Figure 9 reveals that the viscosity increases significantly with increasing solution concentration, while surface tension decreases gradually. Moreover, the electrical conductivity of the SAN solution marginally increases from 3.3 to 6.8 μS/cm with increasing DMF content, because it has a high dipole moment (3.82 Debye) and dielectric constant (37.3) compared to the other ones (Table 1). This indicates that electrical conductivity has a very slight effect on fiber formation from SAN solution. The addition SAN in the solvent increases the electrical conductivity, because, the presence of nitrile group in them increases the ionic/charge movements. It is akin to PAN, which is used in ion exchange membranes.

According to the SEM images shown in Fig. 10, the number of sphere-shaped beads and their size steadily decreased, and as the solution concentration was increased from 8 to 12 %, spindle-like bead structures formed due to low solution viscosity, which resulted in destabilization of the electrified jet. At a flow rate

of 300 µL.h^{-1}, the quantity of polymer solution delivered to the tip of the spinneret is not enough; therefore, beads with non-uniform fibers were formed from solutions of concentrations 12 and 15 %. Nanofibers spun at a concentration of 20 % contain *(C > Ce)*, very few beads when compared to those obtained from a solution of lower concentration; however, the $D_{avg.}$ of the electrospun fibers electrospun was around 280 nm.

3.4 Electrospinning of SAN from toluene

Toluene was able to dissolve SAN to form a spinnable solution, but the continuous spinning of the SAN solution in toluene was very difficult. Because, it has a very low dipole moment (0.36 Debye; Table 1) and a low dielectric constant (2.4; Table 1) compared to the other solvent used. The variations of surface tension, electrical conductivity and coefficient of viscosity as a function of the SAN solutions in toluene are shown in Fig. **11**. It shows that electrical conductivity of the SAN solution marginally increases as their solution concentration increases. Also, the surface tension of the SAN solution was found to be higher than that of pure toluene. As the solution concentration increases, the surface tension values decrease. Thus, the electrical conductivity of the SAN solution does not have a significant effect on the fiber morphology.

By electrospinning of the SAN solution with a lower concentration (≤ 12 %), very small amount of as-spun SAN fibers was obtained, as shown in Fig. **12**. By further increasing the solution concentration to 15 and 20 %, the amount of fibers was found to markedly increase with an average fiber diameter in the range of 400 nm to 1 µm.

3.5 Electrospinning of SAN from 1,2-dichloroethane

1,2-dichloroethane was able to dissolve SAN to form a spinnable solution within 6 h. Figure **13** shows variation of surface tension, electrical conductivity and coefficient of viscosity as a function of the SAN solutions in DCE. As expected, the solution viscosity and conductivity increases significantly with increasing solution concentration, while surface tension decreases gradually. Here, the tip of the nozzle often got clogged by the dried polymer because of the low boiling point of DCE (84.0 °C; Table 1). This clogging is similar to that noticed for the solution of SAN in chloroform and THF.

11

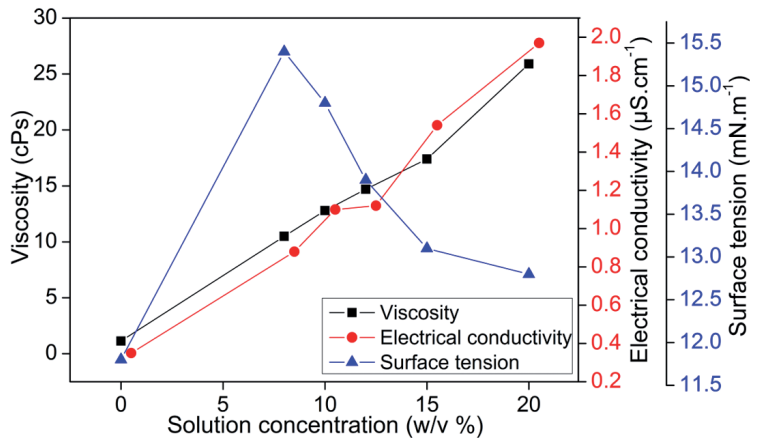

Fig. 11: Variation of coefficient of viscosity, electrical conductivity and surface tension as a function of solution concentration on SAN/toluene solutions.

12

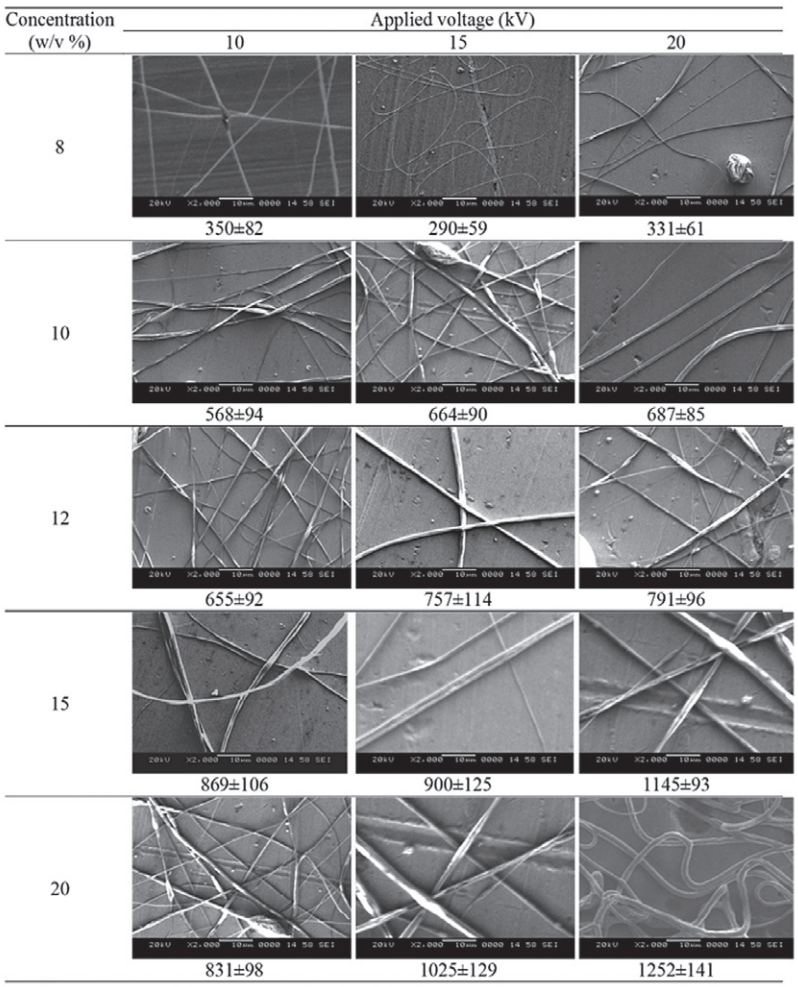

Fig. 12: Representative SEM images (magnification 2000× and scale bar = 10 µm) of SAN fibers spun from toluene solutions of different concentrations (w/v %) under varying applied voltage (for a fixed flow rate of 300 µL h^{-1} and TCD of 23 cm). (The values below the SEM images show the $D_{avg.}$ and the standard deviation of fiber diameter).

13

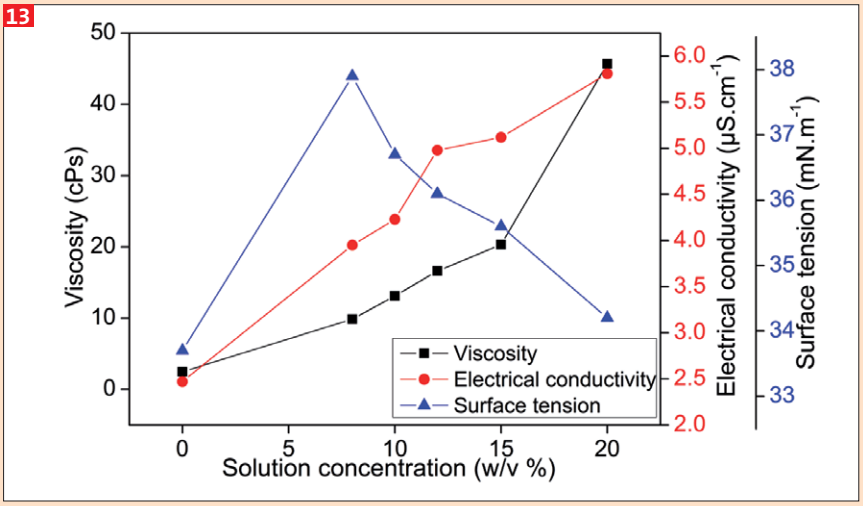

Fig. 13: Variation of coefficient of viscosity, electrical conductivity and surface tension as a function of solution concentration on SAN/DCE solutions.

14

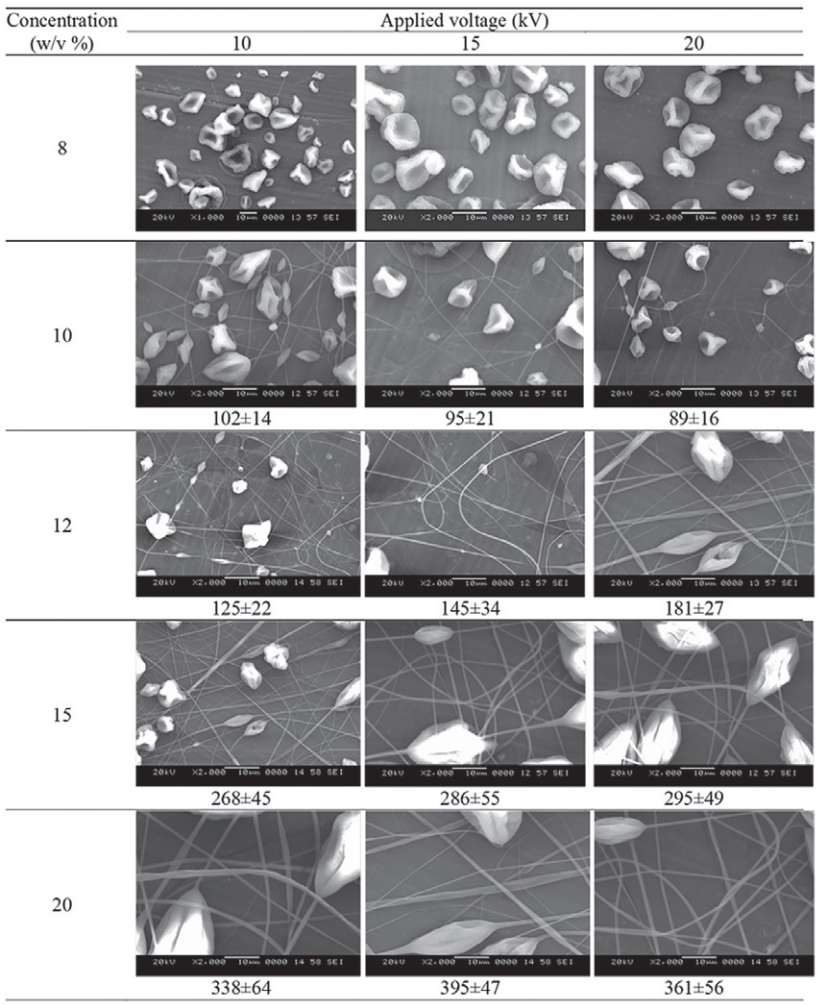

Fig. 14: Representative SEM images (magnification 2000× and scale bar = 10 µm) of SAN fibers spun from toluene solutions of different concentrations (w/v %) under varying applied voltage (for a fixed flow rate of 300 µL h^{-1} and TCD of 23 cm). (The values below the SEM images show the $D_{avg.}$ and the standard deviation of fiber diameter).

SEM micrographs of electrospun SAN fibers are shown in Fig. **14**. It shows that the number of dimple-like beads decreases with increasing the solution concentration from 8 to 12 %. At low concentrations (≤12%), electrospun SAN fibers are harder to dry before they reach the collector plate. Furthermore, the presence of high solvent content of the solution jet favors the formation of beads along with electrospun fibers. As the solution concentration was increased beyond the C_e (15%), beaded nanofibers were produced, which indicates that there are no entanglements between polymer chains in solutions below C_e. For the electrospun fibers with 20 % solutions of SAN, spindle-like beaded fibers were observed. It was found that the varied applied voltage and flow rate marginally controlling the fiber morphology and diameter.

3.6 Electrospinning of SAN from n-butanone

n-butanone was able to dissolve SAN to form a spinnable solution within 6 h. The variations of surface tension, electrical conductivity and coefficient of viscosity as a function of the SAN solutions in MEK are shown in Fig. **15**. As shown in Fig. 15, the electrical conductivity and viscosity of the SAN solution increase as the solution concentration increases. Increase in either of these parameters leads to the formation of defect-free, uniform SAN fibers. Moreover, gradually decrease in surface tension plays a vital role in determining the range of SAN solution concentration from which continuous stable jet can be obtained in electrospinning.

The SEM micrographs of electrospun SAN fibers attained from solutions in the concentration range of 10–25 w/v % are shown in Fig. **16**. Numerous dimple and cups-like beads were noticed among the electrospun fibers, particularly those originating from 8, 10 and 12 % SAN solutions. Once the solution concentration increased to 15 %, the number of beads decreased due to the onset of entanglement couplings between chains in the polymer solution. When the solution concentration increased to above 15 %, bead-free fibers were obtained and fibers became thicker.

3.7 Electrospinning of SAN from ethylacetate

Ethylacetate was able to dissolve SAN to form a spinnable solution. The solution got clogged at the tip of the spinneret

and also lesser amount of the fibers was produced at all concentrations of the solution, possibly due to the fast evaporation of the solvent (cf. the low boiling point of ethyl acetate of 77.1 °C), as shown in Table 1. Figure 17 illustrates the variations of surface tension, electrical conductivity and coefficient of viscosity as a function of the SAN solutions in EA. It shows that the electrical conductivity increases as the solution viscosity and concentration increases from 8 to 20 %. The reason could be the higher dielectric constant (6.4; Table 1) of the solvent system.

Figure 18 shows the SEM micrographs of the electrospun SAN fibers obtained from solutions of different concentrations. At low solution concentrations (≤12 %), relatively large amount of discrete mushroom-like beads and beaded fibers were observed. The structure of the mushroom-shaped cross-sectional SAN fibers could be a reason for the collapsing of the charged jet upon evaporation of the solvent. The beaded fiber morphology completely eliminated when the solution concentration was about 20 %. Moreover, the D_{avg} of the electrospun SAN fibers increases monotonically with increasing the solution concentration.

3.8 Electrospinning of SAN from dimethlysulfoxide

Dimethlysulfoxide was able to dissolve SAN to form a spinnable solution to fabricate SAN fibers. Ultrafine SAN nanofibers could be easily spun from DMSO solution. This is due to the very high dielectric constant (46.7; Table 1) and dipole moment (3.96 Debye; Table 1) of the solvent. The variations of surface tension, electrical conductivity and coefficient of viscosity as a function of the SAN solutions in DMSO are shown in Fig. 19. Figure 19 shows that viscosities of the SAN solutions increase exponentially with increasing solution concentration from 8–20 %, while surface tension decreases gradually. Moreover, a slight increase in the electrical conductivity of the SAN solution does not have a significant effect on the diameter of electrospun SAN fibers.

Figure 20 shows the SEM images of the electrospun SAN fibers obtained at different solution concentrations (8–20 %) and at varied applied voltage from 10–20 kV. The smallest D_{avg} of spindle-like beaded fibers were obtained, from SAN solutions of low concentration (8

15

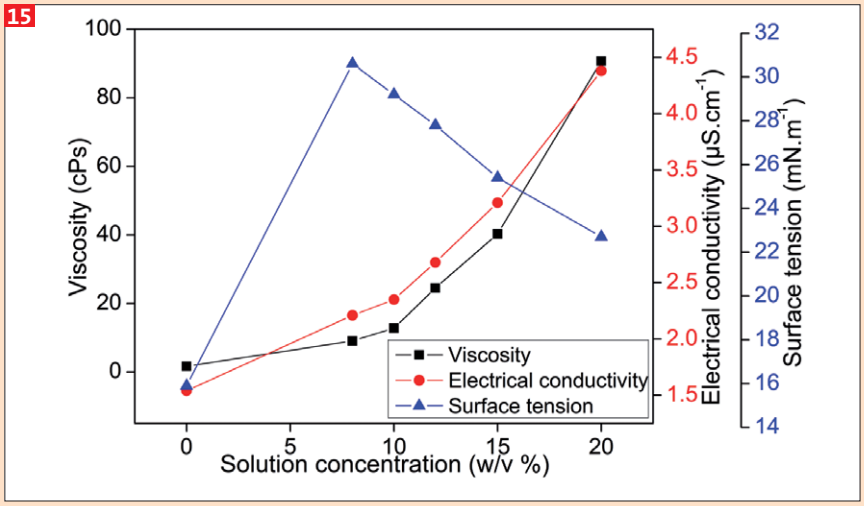

Fig. 15: Variation of coefficient of viscosity, electrical conductivity and surface tension as a function of solution concentration on SAN/MEK solutions.

16

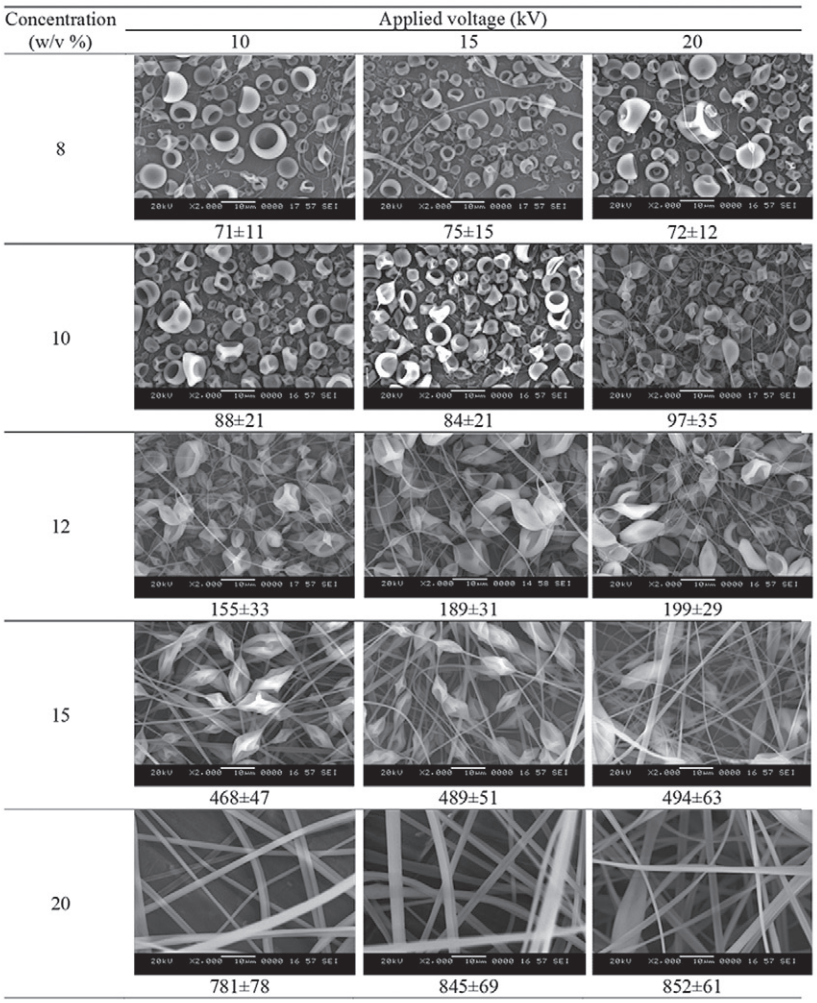

Fig. 16: Representative SEM images (magnification 2000× and scale bar = 10 µm) of SAN fibers spun from MEK solutions of different concentrations (w/v %) under varying applied voltage (for a fixed flow rate of 300 µL h^{-1} and TCD of 23 cm). (The values below the SEM images show the $D_{avg.}$ and the standard deviation of fiber diameter).

17

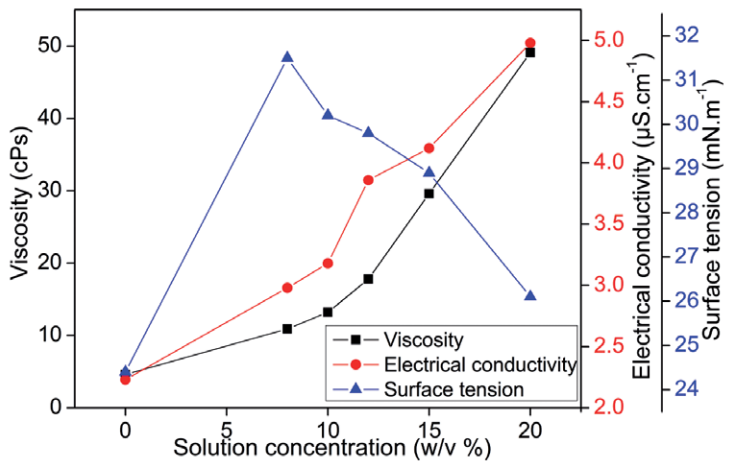

Fig. 17: Variation of coefficient of viscosity, electrical conductivity and surface tension as a function of solution concentration on SAN/EA solutions.

18

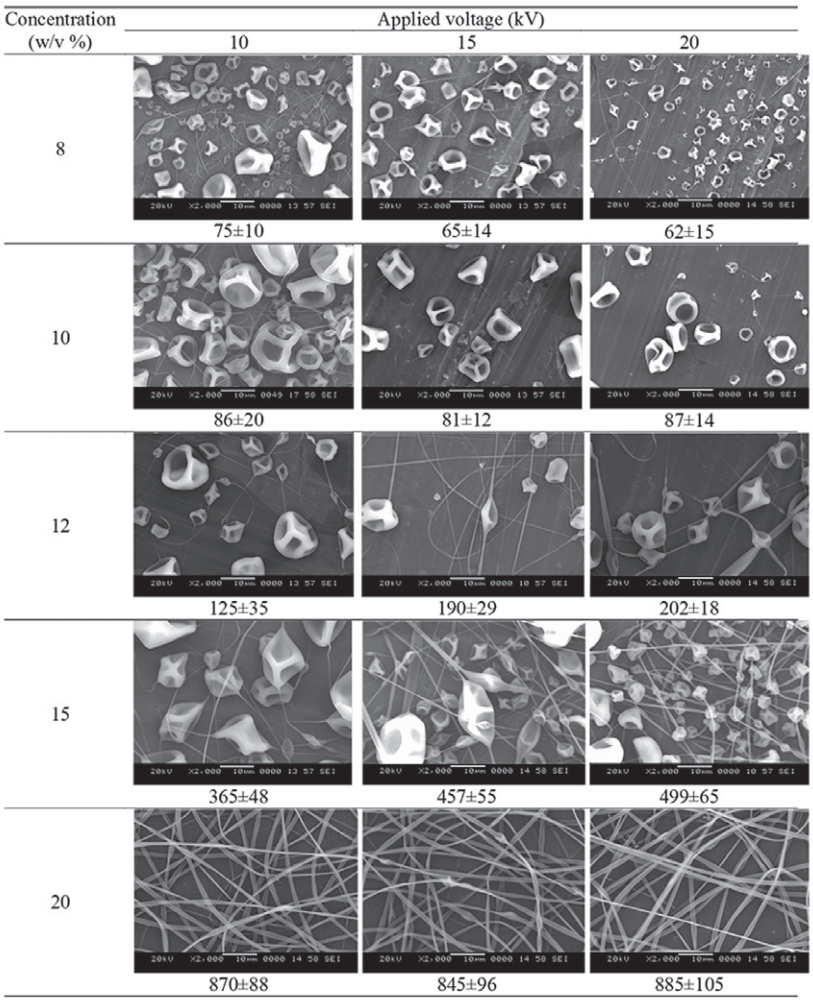

Fig. 18: Representative SEM images (magnification 2000× and scale bar = 10 µm) of SAN fibers spun from EA solutions of different concentrations (w/v %) under varying applied voltage (for a fixed flow rate of 300 µL h^{-1} and TCD of 23 cm). (The values below the SEM images show the $D_{avg.}$ and the standard deviation of fiber diameter).

and 10%), since the boiling point of DMSO is relatively high (192 °C; Table 1), thereby the charged jet did not have sufficient time to dry during its reach to the collector plate. At 12 %, larger amount of fibers with occasional presence of beads were observed. When the solution concentration was increased to 15 %, uniform fibers along with fewer beads were obtained due to the higher number of entanglements. With a further increase in the polymer concentration (20 %), ultrafine bead-free fibers with an of $D_{avg.}$ 800 nm were formed. A higher applied voltage (≥15 kV) resulted in superior stretching of the polymer solution due to the better Columbic forces in the charged jet as well as electric field; these effects favor rapid evaporation of solvent from the electrospun fibers.

From the detailed analysis of the fibers obtained using different solvents, DMSO, DMF and MEK were found to produce SAN nanofibers with good morphological features. The properties of the solvents such as boiling point, dielectric constant and dipole moment played in the production of bead-free fibers. Figure 21 compares the aforesaid properties of the solvents. It is observed that, for the solvents DMSO, DMF and MEK, the values of these physical properties are the highest and they are considered to be the best for the electrospinning of SAN for a solution concentration of 20 w/v%. As these properties are reduced, the morphology of the fibers obtained from the respective solvents at the maximum solution concentration (20 w/v%) were nanofibers with intermittent beads. The dielectric constant of the solvent has a crucial role in electrospinning process, since the transformation of beaded to bead-less fibers is observed as the solvent is changed from 1,2-dichloroethane to n-butanone. These solvents have more-less closely matching physical properties except the dielectric constant. Therefore, the minimum dielectric constant required by the solvent for the successful electrospinning of SAN corresponds to that of n-butanone. The morphology of the fibers obtained at 20 w/v% of SAN in 1,2-dichloroethane is similar to the case of best solvents at a lower solution concentration (15 w/v%). Therefore, it is expected that, bead-free fibers can be obtained if we can increase the concentration of SAN in the solvent (>20 w/v%), since the addition of more SAN can increase the dielectric constant of the spinning solution.

4. Conclusions

Hansen solubility parameter and Teas plot were used to choose a solvent for electrospinning of poly(styrene-*co*-acrylonitrile). Among the eight solvents studied, only the SAN solutions in DMSO, DMF and MEK were found to produce SAN nanofibers with good productivity and with satisfactory morphological appearance, while the SAN solutions in CF, THF, toluene, DCE and EA were not significantly spinnable. Based on the qualitative observation of the results obtained, the physical constants of the solvents such as boiling point, dipole moment and dielectric constant greatly influence the electrospun SAN fiber morphology. Also, the best fiber morphology is mainly due to the increase in solution viscosity, which is due to the increase in solution concentration and, increase in electrical conductivity and reduction in surface tension complimented the increase in the viscosity and the variations are negligibly small with respect to viscosity. Notably, the solution viscosity was found to play a governing role in determining the behavior of the solution jet during the electrospinning process. Consequently, there was an optimal solvent system, which could almost eliminate beads in electrospun webs, and the efficiency of the electrospinning process also strongly depended upon the chosen solvent system.

Acknowledgements

T. Senthil would like to thank the department of Metallurgical and Materials Engineering, National Institute of Technology of Karnataka (NITK), India for a research fellowship. Ms. U. Rashmi is gratefully acknowledged for her kind assistance in scanning electron microscopy.

References

[1] Wang, X., Ding, B., Li, B. Mater. Today. **16**, 229 (2013).
[2] Faccini, M., Vaquero, C., Amantia, D., J. Nanomater. 2012, 1-9 (2012).
[3] Cho, H., Min, S.-Y., Lee, T.-W., Macromol. Mater. Eng. **298**, 475 (2013).
[4] Desai, K., Kit, K., Li, J., Michael Davidson, P., Zivanovic, S., Meyer, H., Polymer. **50**, 3661 (2009).
[5] George, G., Elias, L., Hegde, A.C., Anandhan, S. RSC Adv. **5**, 40940 (2015).
[6] Amna, T., Hassan, M.S., Barakat, N.A.M., Pandeya, D.R., Hong, S.T., Khil, M.-S., Kim, H.Y., Appl. Microbiol. Biotechnol. **93**, 743 (2011).
[7] Senthil, T., Anandhan, S., J. Colloid Interf. Sci. **432**, 285 (2014).

19

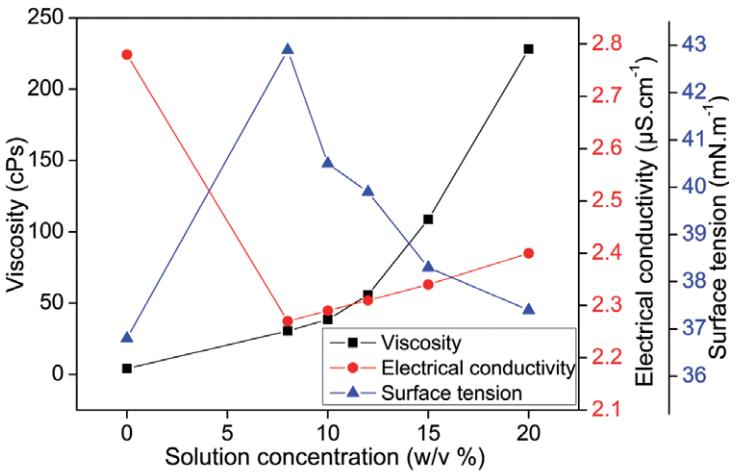

Fig. 19: Variation of coefficient of viscosity, electrical conductivity and surface tension as a function of solution concentration on SAN/DMSO solutions.

20

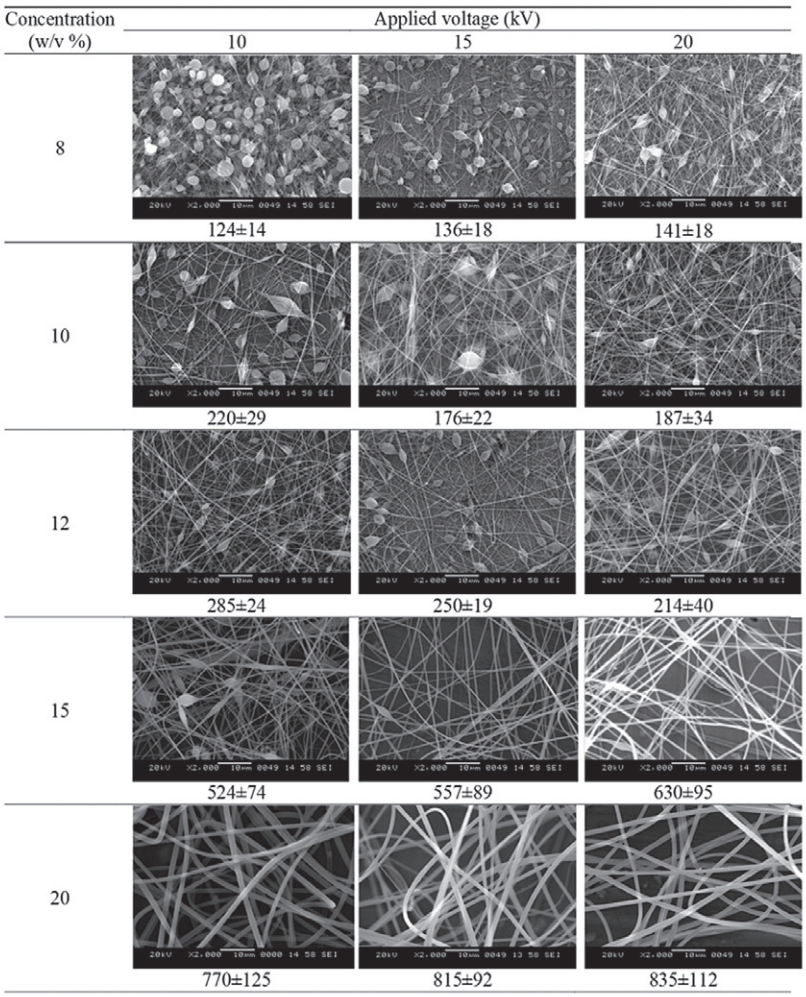

Fig. 20: Representative SEM images (magnification 2000× and scale bar = 10 μm) of SAN fibers spun from DMSO solutions of different concentrations (w/v %) under varying applied voltage (for a fixed flow rate of 300 μL h^{-1} and TCD of 23 cm). (The values below the SEM images show the $D_{avg.}$ and the standard deviation of fiber diameter).

21

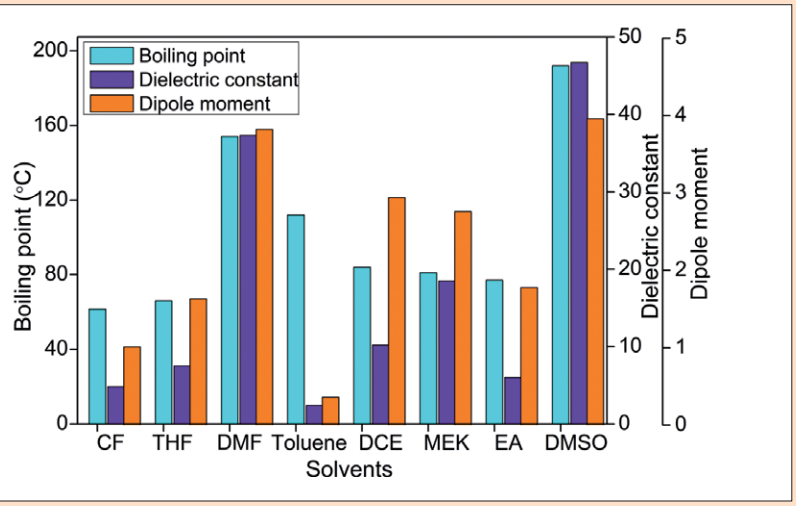

Fig. 21: Variation of boiling point, dielectric constant and dipole moment as a function of solvents.

[8] Huang, Z.-M., Zhang, Y.-Z., Kotaki, M., Ramakrishna, S, Compos. Sci. Technol. **63**, 2223 (2003).
[9] Reneker, D.H., Yarin, A.L., Fong, H., Koombhongse, S., J. Appl. Phys. **87**, 4531 (2000).
[10] Pillay, V., Dott, C., Choonara, Y.E., Tyagi, C., Tomar, L., Kumar, P., du Toit, L.C., Ndesendo, V.M.K., J. Nanomater. 2013, 1–22 (2013).
[11] Yördem, O.S., Papila, M., Menceloğlu, Y.Z., Mater. Design. **29**, 34 (2008).
[12] Luo, C.J., Nangrejo, M., Edirisinghe, M., Polymer. **51**, 1654 (2010).
[13] Li, L., Li, R., Li, M., Rong, Z., Fang, T., RSC Adv. **4**, 27914 (2014).
[14] Luo, C.J., Stride, E., Edirisinghe, M, Macromolecules. **45**, 4669 (2012).
[15] Haas, D., Heinrich, S., Greil, P. J. Mater. Sci. **45**, 1299 (2009).
[16] Jarusuwannapoom, T., Hongrojjanawiwat, W., Jitjaicham, S., Wannatong, L., Nithitanakul, M., Pattamaprom, C., Koombhongse, P., Rangkupan, R., Supaphol, P., Eur. Polym. J. **41**, 409 (2005).
[17] McKee, M.G., Wilkes, G.L., Colby, R.H., Long, T.E., Macromolecules. **37**, 1760 (2004).
[18] Hansen, C.M.: Hansen Solubility Parameters: A User's Handbook, Second Edition. CRC Press Inc, Boca Raton, Florida (2007).
[19] Barton, A.F.M.: Handbook of Solubility Parameters and Other Cohesion Parameters, Second Edition. CRC Press Inc, Boca Raton, Florida (1991).
[20] Seymour, R.B.: Engineering Polymer Sourcebook. McGraw-Hill, New York (1990).
[21] Kim, M.-J., Kang, E.-S., Park, D.-W., Shim, B.-S., Shim, S.-E., Bull. Korean Chem. Soc. **33**, 2867 (2012).
[22] Jianxiang, Y.U., Taiqi, L.I.U., Acta. Polymerica. Sinica. **6**, 514 (2007).
[23] Gudkova, V., Krumme, A., Märtson, T., Rikko, M., Tarassova, E., Viirsalu, M., J. Electrostat. **72**, 433 (2014).
[24] Brandrup, J., Immergut, E.H.: Polymer Handbook. John Wiley & Sons, New York (1989).
[25] Smallwood, I.M.: Solvent Recovery Handbook, Second Edition. Blackwell Science, CRC Press, New York (2002).
[26] Wannatong, L., Sirivat, A., Supaphol, P., Polym. Int. **53**, 1851 (2004).
[27] Teas, J.P., J. Paint Technol. **40**, 19 (1968).
[28] Pelofsky, A.H., J. Chem. Eng. Data. **11**, 394 (1966).

Compounds für Anwendungen im Automobil-Innenraum

COMPOUNDS An Kunststoffteile im Automobil-Innenraum werden höchste Ansprüche gestellt. Hier sind unter anderem allgemeine Produktqualität, Farbkonstanz sowie Beständigkeit gegen gängige Heißlichtalterungstests der Automobilindustrie zu nennen. Bada, Bühl, bringt nun eine Vielzahl neuer Produktlösungen auf den Markt, die diesen Ansprüchen gerecht werden. Compounds auf Basis Polyamid 6 mit variabler Glasfaserverstärkung vereinen eine hohe Beständigkeit gegen Heißlichtalterung mit sehr guten mechanischen Eigenschaften und individueller Einfärbung. Badamid B70 GF30 H UV ist ein langjährig bewährtes Beispiel für diese Produktklasse und eignet sich bestens für Sichtteile mit hohen mechanischen Anforderungen, die dauerhaft der Sonnenstrahlung ausgesetzt sind. Polymerblends aus ASA+PC genießen einen immer höheren Stellenwert im Interieur. Hohe Lichtbeständigkeit, antistatische Eigenschaften gegen Staubablagerungen und Lieferung in gängigen Automobilfarben ermöglichen die Herstellung von Bauteilen im direkten Einstrahlbereich der Sonne. Badalac ASA/PC 120 H UV AS besteht gängige Tests der Automobilindustrie hinsichtlich Heißlichtalterung und Ableitfähigkeit und findet beispielsweise Anwendung in Ablagefächern und Schiebeelementen. Thermoplastische Elastomere TPE-S sind ebenfalls mit hoher UV-Beständigkeit, antistatisch und eingefärbt lieferbar. Optional kann die Dichte dieser Compounds auf <0,8 g/cm³ gesenkt werden. Für Badaflex TPE-S 60A 5471LD AS eröffnen sich hierdurch weite Anwendungsfelder, wie beispielsweise Ablagematten und Griffe, die zusätzlich mit geringerem Teilegewicht hergestellt werden können. TPE-S Compounds mit 2K-Haftungsmodifizierung bilden einen wichtigen Spezialitätenbereich im Portfolio ab. Badaflex TPE-S 60A 5206 UV 2K haftet besonders gut auf ABS, ABS/PC sowie ASA/PC-Blends und besteht Heißlichtalterungstests sowohl in feucht- und trocken-heißem Klima. Dieses Compound ist daher zusätzlich im Außenbereich einsetzbar. Badaflex TPE-S 35A 5455 2K bietet eine hervorragende Haftung auf dem weit verbreiteten Werkstoff Polyamid 6, was weitere Konstruktionsmöglichkeiten eröffnet. Alle Typen sind in einem weiten Härtebereich lieferbar und eignen sich für 2K-Spritzlinge.

KONTAKT
Bada, Bühl,
Tel. +49 7223 9407 70